NACA TM 1441

TECH LIBRARY KAFB, NM
0144571

# NATIONAL ADVISORY COMMITTEE FOR AERONAUTICS

TECHNICAL MEMORANDUM 1441

7990

## THE EFFECT OF FREE-STREAM TURBULENCE ON HEAT TRANSFER FROM A FLAT PLATE

By Sugao Sugawarā, Takashi Sato, Hiroyasu Komatsu, and Hiroichi Osaka

Translation of "Shuryūbu midare ga heiban nets udentatsu ni oyobosu likyō ni tsuite," Jour. Jap. Soc. Mech. Eng., vol. 19, no. 18, 1953, pp. 18-25.

Washington

September 1958

TECH LIBRARY KAFB, NM
0144571

4826

CD-1

NATIONAL ADVISORY COMMITTEE FOR AERONAUTICS

TECHNICAL MEMORANDUM 1441

# THE EFFECT OF FREE-STREAM TURBULENCE ON HEAT TRANSFER FROM A FLAT PLATE*

By Sugao Sugawara, Takashi Sato,
Hiroyasu Komatsu, and Hiroichi Osaka

The effect of initial turbulence on the surface heat transfer was investigated in the case of a smooth flat plate. The initial turbulence was introduced by a screen, and the percentage turbulence $\sqrt{\overline{u^2}}/U$ was measured accurately by a hot-wire anemometer in the boundary layer and in the main flow. On the other hand, the change of the temperature difference between air and a plate, during the plate's being cooled, was measured in the same condition, and from its result the local heat-transfer coefficient on the surface was calculated.

Thus, we were able to make clear the relation between initial turbulence and heat transfer. Surface heat transfer becomes better with the enlargement of the initial turbulence, and the increasing of heat-transfer coefficient was remarkable within the range of small initial turbulence. In the rage of larger initial turbulence than 7 to 8 percent, the local heat-transfer coefficient increased no more, and its value was 55 percent larger compared with the case of the smallest initial turbulence.

## 1. INTRODUCTION

Surface heat transfer is a phenomenon of heat exchange through the boundary layer surrounding the surface of a solid body, it is natural, therefore, that the factors affecting the condition of boundary layer also influence heat-transfer phenomena. It is considered that turbulence existing in the main flow will influence the boundary layer and, therefore, surface heat transfer. Many investigations of surface heat transfer have been conducted in which very little or no turbulence exists in the main flow, or without consideration of any turbulence that may be present. However, in many practical situations, comparatively strong turbulence is present and, therefore, should be taken into account.

---

*"Shuryūbu midare ga heiban nets udentatsu ni oyobosu likyō ni tsuite," Jour. Jap. Soc. Mech. Eng., vol. 19, no. 18, 1953, pp. 18-25.

Experimental results that were made to clarify the effect of such turbulence on heat transfer at the surface of a smooth flat plate are reported herein. The turbulence was generated by screens in the wind tunnel, and the turbulence percentage $\sqrt{\overline{u^2}}/U$ was measured accurately by a hot-wire anemometer both in the boundary layer and the free stream.

## 2. EXPERIMENTAL APPARATUS AND METHOD

### i.

4826

The main apparatus as shown in figure 2 was the same as that described in reference 1. An apparatus to generate various degrees of turbulence was added as shown in figure 1. It consists of a screen S behind the tunnel inlet T, built by connecting a number of circular rods in a square array. The important dimensions of the rods are given in the following table:

TABLE 1. - SCREEN DIMENSIONS, mm

| Screen | A | B | C |
|---|---|---|---|
| Rod diameter | 6 | 3 | 1 |
| Rod pitch | 28 | 13 | 7 |

The turbulence generated was the strongest when using arrangement A and the weakest with C. A smooth flat plate P was suspended in a duct M. Since the turbulence induced by the screen decreases with increasing distance from the screen, the turbulence near the measuring plate P can be adjusted by varying the relative position of the screen and the plate. This screen-to-plate distance is changed by an insert duct D between the screen and the plate which had a length of either 50 or 10 centimeters. Experiments were carried out by combining two lengths of D, or without D, with three kinds of S.

### ii. [sic] Heat Transfer Coefficient Measurements

The method of measurement was the same as described in reference 1. The local heat-transfer coefficient $\alpha$ is calculated from the relation

$$\alpha = Bc\gamma s/2 \tag{1}$$

where $c$, $\gamma$, and $s$ are specific heat, specific weight, and thickness of a plate, respectively. The constant $B$ multiplies the time $t$ in the equation of temperature difference between the plate and air

$\theta$, as defined by

$$\theta = Ae^{-Bt} \tag{2}$$

B was determined from the relation between $\theta$ and t which was measured directly by two millivolt meters. Local heat transfer coefficients were measured at twelve locations along the plate, and two values of free-stream velocity were used (14 m/sec and 7 m/sec).

4826

CD-1 back

### iii. Measurement of Turbulence Strength

(a) Frequency characteristics of amplifier used to measure turbulence. - A hot-wire anemometer was used for the measurement of turbulence. With this type of sensing element, the frequency response is limited by the heat capacity of the hot wire. That is, the temperature variations of the hot wire which are read as voltage variations between the terminals do not follow the velocity variations of the flowing fluid, and both amplitude attenuation and phase shift are present. Moreover, both of these effects become greater as the frequency increases. From reference 2, the amplitude decrease is proportional to $1/\sqrt{1 + (M\omega)^2}$, and the phase shift is proportional to $\tan^{-1}M\omega$, where $\omega = 2\pi f$, with f as the frequency and $M = 4.2\ \rho A^2 c(\overline{T} - T_0)/i^2 r$ proportional to the heat capacity of the hot wire, $\rho$, A, c, and r are specific resistance, cross-sectional area, specific heat, and resistance of the hot wire, respectively, $\overline{T}$ and $T_0$ are mean temperatures of the hot wire and fluid, respectively, and i is the current through the hot wire.

Such amplitude attenuations and phase shifts must be compensated since turbulence is distributed over a frequency spectrum. In order to accomplish this compensation, the characteristics of the amplifier must be the reverse of those of the hot wire.

The compensating method used in the amplifier utilized negative feedback as described in reference 3. The circuit diagram is shown in figure 2. Negative feedback is accomplished from the plate of $V_3$ to the cathode of $V_2$.

$$\dot{G}(\dot{E}_i + \dot{E}_0\dot{\beta}) = \dot{E}_0$$

where $\dot{G}$ is the amplification of $V_2$ and $V_3$, $\dot{\beta}$ is the amount of negative feed-back, $\dot{E}_i$ is the input voltage of $V_2$, and $\dot{E}_0$ is output voltate of $V_e$. Therefore,

$$\dot{E}_0/\dot{E}_i = \dot{A} = \frac{\dot{G}}{1 - \dot{\beta}\dot{G}}$$

where $\dot{A}$ is the actual amplification including negative feedback. Specially, when $|\dot{G}\dot{\beta}| >> 1$,

$$\dot{A} \cong -\frac{1}{\dot{\beta}} \tag{3}$$

Referring to figure 2, the combined impedance $\dot{z}$ of $R_1$ and $C_1$ is

$$\dot{z} = \frac{R_1}{1 + j\omega C_1 R_1} \qquad j = \sqrt{-1}$$

4826

and if we choose $R_0 >> |\dot{z}|$,

$$\beta = \dot{z}/(R_0 + \dot{z}) \cong \dot{z}/R_0$$

Therefore, from equation (3),

$$\dot{A} = -R_0/\dot{z} = -R_0(1 + j\omega C_1 R_1)/R_1 \tag{4}$$

If we choose the values $C_1$ and $R_1$ as $C_1 R_1 = M$, we can compensate for the decrease of amplitude and phase shift of the hot wire. It will be noted that the characteristics of the amplifier must be as flat as possible when negative feedback is not applied.

A vacuum thermocouple was used for the measurement of the alternative component (turbulent component) of the output voltage. C is a blocking condensor for the constant (nonvariable component) voltage.

Voltage induced in the T-circuit is proportional to $\sqrt{\overline{u^2}}$, where u is variation of velocity (turbulence); a bar over a symbol means an average with respect to time.

Since the diameter of the hot wire used in our experiment was 30 microns and its length was about 10 millimeters, the current passing through a hot wire was adjusted to 300 milliamperes. (The average temperature of the hot wire was about 170° C for a mean flow velocity of 14 m/sec, so that M = 0.023 sec.)

Figure 3 shows the frequency characteristics of our system where the broken line is the theoretical result of combining a hot wire with an amplifier having a perfectly flat characteristic; the circles show the results of combining a hot wire with an amplifier without the negative feedback circuit. The double circles show the output of the T-circuit when a hot-wire anemometer was connected with our amplifier using negative feedback. As shown in figure 3, the curve for the double circles is satisfactorily flat between 20 and 7000 cycles. Figure 4 shows the calibration equipment for determining frequency characteristics.

The calibration for the absolute value of $\sqrt{\overline{u^2}}$ was carried out by using a dynamic speaker. A hot-wire probe was fixed to the moving part of the speaker and the amplitude was measured by a traversing micrometer. The frequency was checked by a tuning fork and standard frequency meter.

(b) Effect of mean velocity. - The sensitivity of a hot-wire may be affected by the change of mean velocity. The relation between the voltage $E$ of the direct current that appears between the hot-wire terminals, and the mean velocity $U$ is not in a straight-line relation as shown in figure 5. This means that the sensitivity of a hot wire is a function of the mean velocity. Namely, its sensitivity must be proportional to $dE/dU$ at the point of $U_1$ when the mean velocity is $U_1$. Therefore, we can make a correction by multiplying the ratio $dU/dE$ by the value at some standard condition where the calibration was made. The relation between $U$ and $E$ depends also on the fluid temperature as shown in figure 5. The broken line in figure 5 shows the value of $dU/dE$ at 18° C. The correction for temperature is necessary, of course, but the change of $dE/dU$ is not as large as the change of temperature, since the curves for variable temperature are approximately parallel.

4826

Figure 6 shows the circuit diagram for the apparatus used to measure the mean velocity. In principle it is a bridge circuit that utilizes a difference method. $R$ is a hot wire and the voltage difference appears between the terminals of $R$ and $R_1$. ($R_1$ is a constant resistance that is scarcely affected by temperature changes.) The currents of the two circuits are kept constant by adjusting $R_0'$ and $R_2'$.

Utilizing the above mentioned, we can measure the value of $\sqrt{\overline{u^2}}/U$ which is the percentage of turbulence.

## 3. DISCUSSION OF RESULTS

### i. Turbulence and Velocity Distributions in the Boundary Layer

Figures 7 and 8 show two examples of the experimental results. The distance from the plate surface is $y$, and $f$, $m$, and $r$ indicate plate position as shown in figure 1. (Front edge of a plate, $f$; middle of a plate, $m$; near rear edge of a plate, $r$.) Figure 7 illustrates the results when no screens are used but with the auxiliary duct D. Consequently, the turbulence is comparatively small. Figure 8 shows the result of using screen A but without duct D, and is indicative of the effect of strong turbulence in the main flow. Broken lines in both figures show $\sqrt{\overline{u^2}}/U$, with $U$ the local mean velocity at $y$. The full lines show $\sqrt{\overline{u^2}}/U_0$ where $U_0$ is the constant mean velocity of the main flow (approximately 14 m/sec in the case of fig. 7 and 12 m/sec in the case of fig. 8). At the positions $m$ and $r$, the boundary layers were turbulent in both

cases. The value of $\sqrt{\overline{u^2}}/U$ reaches a maximum value of one-third or one-fourth of the boundary-layer thickness, and its value is larger in the case of figure 8 than in figure 7. The thickness of the boundary layer is considerably greater in the case of figure 8. By comparing those two figures, we can recognize that the percent of turbulence in the boundary layer becomes larger through the increase of the turbulence level of the main flow; at the same time, the thickness of the laminar sublayer becomes smaller. (This is also apparent in figs. 9 and 10.) Figures 9 and 10 show the time - mean velocity distribution in the boundary layer in the same cases as figures 7 and 8. Open circles show the results for the case of figure 7, and solid circles show those of figure 8. The thickness of the boundary layer $\delta$ was determined as the value of $y$, where the velocity was 99.5 percent of the main-flow velocity.

4826

## ii. Heat-Transfer Results

Figures 11 and 12 show heat-transfer results. Those figures show the relation between Nusselt number Nu and Reynolds number Re in a few cases of variable turbulence, where

$$Nu = \alpha x/\lambda \qquad Re = U_0 x/\nu$$

and $\alpha$ is the local heat-transfer coefficient at a distance $x$ from the front edge.

Figure 11 shows the case for screen A with a duct length D of 50 centimeters; the influence of the mean velocity of the main flow is shown. There is no appreciable effect of mean velocity on the relation between Re and Nu, which is similar to the case of low main-stream turbulence. Laminar heat transfer is shown as a square-root relation, $Nu = 0.425\ Re^{0.5}$. In the laminar boundary-layer range the effect of turbulence is not so remarkable, but the transition Re from laminar to turbulent flow decreases as the turbulence in the main flow increases. Over the entire range of main-flow turbulence studied, the relation between Nu and Re can be expressed as follows for the range of turbulent heat transfer:

$$Nu = KRe^{0.8} \tag{5}$$

This slope is the same as the case that includes very small turbulence in main flow, i.e., the straight lines that represent the relation of turbulent heat transfer are parallel to each other as shown in figures 11 and 12. The value of Nu increases according to the increase of main-stream turbulence. In other words, the value of K in equation (5) increases with the increase of turbulence in the main flow. Figure 13 shows the relation between percent of main-stream turbulence and the increase of

Nu. The abscissa is $(Nu - Nu_0)/Nu_0$, where $Nu_0$ is the value of Nu in the case of the smallest turbulence (percentage turbulence was 0.37 percent) in our experiments and the relation between $Nu_0$ and Re is shown as follows:

$$Nu_0 = 0.0194\ Re^{0.8} \tag{6}$$

The coordinate of figure 13 is the percentage turbulence in the main flow near the front edge of the plate (point f in fig. 1). The main flow turbulence decreases in the flow direction in this case, so it is difficult to determine the position of turbulence to be used for such figures. It is noted that the turbulence near the transition point affects mainly the turbulent boundary layer heat transfer. It is difficult, however, to determine the transition point exactly and moreover, the transition point existed comparatively near the front edge in these experiments since the form of the front edge was flat and not sharp. Therefore, the turbulence near the front edge is used in figure 13 for convenience. The following table shows the result of decreasing the turbulence in the main flow.

4826

TABLE 2

| Length of duct D, cm | | None | None | 50 | None |
|---|---|---|---|---|---|
| Kind of screen | | None | A | A | B |
| Decrease of turbulence in main flow, percent | | | | | |
| Position f | [NACA note: see fig. 1] | 0.75 | 7.42 | 2.05 | 3.54 |
| Position m | | 0.72 | 4.85 | 1.53 | 2.68 |
| Position r | | 0.75 | 3.58 | 1.32 | 1.78 |

As shown in figure 13, Nu increases with increasing turbulence, and the rate of increase is larger in the low turbulence range than in the high turbulence range. In the range larger than 7 to 8 percent turbulence, Nu becomes almost constant. The maximum increase of Nu was 55 percent.

The inclination of such changes is very similar to the results reported by Comings, et al. (ref. 4) for the case of flow perpendicular to a circular cylinder. In their experimental results, Nu did not change any more in the range between 7 and 22 percent. We cannot, however, quantitatively compare our results with theirs, since not only are the geometries different, but also the then-reported mean heat-transfer coefficients, including the laminar heat-transfer range.

## 4. CONCLUSIONS

In order to study the effect of main-stream turbulence on the surface heat transfer in the case of forced convection along the flat plate, experiments were carried out by changing the main-stream turbulence through the use of screens and settling sections. The results obtained are summarized as follows:

i. The transition Reynolds number from laminar to turbulent flow decreases as the main-stream turbulence level increases.

ii. Increasing the turbulence of the main flow, increases the turbulence level in the turbulent boundary layer, and decreases the thickness of the sublayer. This causes an increase in the heat-transfer coefficient.

iii. In the range of laminar heat transfer, the effect of turbulence in main flow was not great. In the range of turbulent heat transfer, the heat-transfer coefficient increases according to the increase of turbulence, but Nu was still proportional to $Re^{0.8}$.

iv. Nu increases sharply in the smaller turbulence range, and the increase becomes gradual in the range of larger turbulence. Nu is almost constant in the range of turbulence larger than 7 to 8 percent. The maximum value of Nu was 55 percent larger than the minimum value of Nu.

## REFERENCES

1. Sugawara, S., and Sato, T.: Memoirs of Faculty of Engineering. Kyoto Univ., vol. 14, no. 1, 1952. (See also Trans. Japan Soc. Mech. Eng., vol. 17, no. 62, 1951, p. 122.)

2. Dryden, H. L., and Kuethe, A. M.: The Measurement of Fluctuations of Air Speed by the Hot-Wire Anemometer. NACA Rep. 320, 1929.

3. Tanekoda: Rep. of Inst. of Fluid Dynamics (Kyushu Univ., Japan), vol. 7, no. 3, 1951, p. 18.

4. Comings, E. W.; Adams, C. H., and Shippee, E. D.: High Velocity Vaporizers. Ind. and Eng. Chem., vol. 40, no. 1, Jan. 1948, pp. 74-76.

Translated by
Takashi Sato
University of Minnesota
Institute of Technology
Mechanical Engineering Department

4826

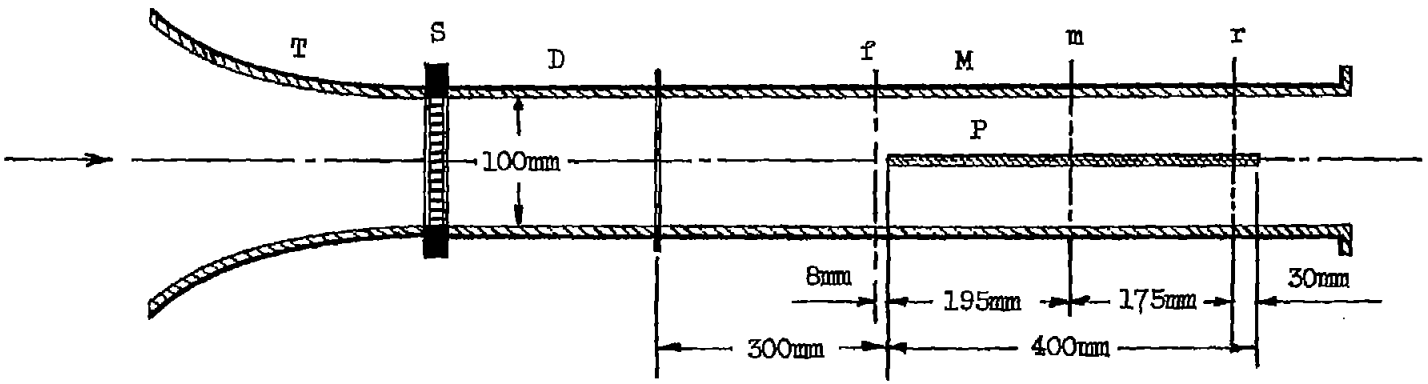


Figure 1. - Experimental apparatus to generate various degrees of turbulence.

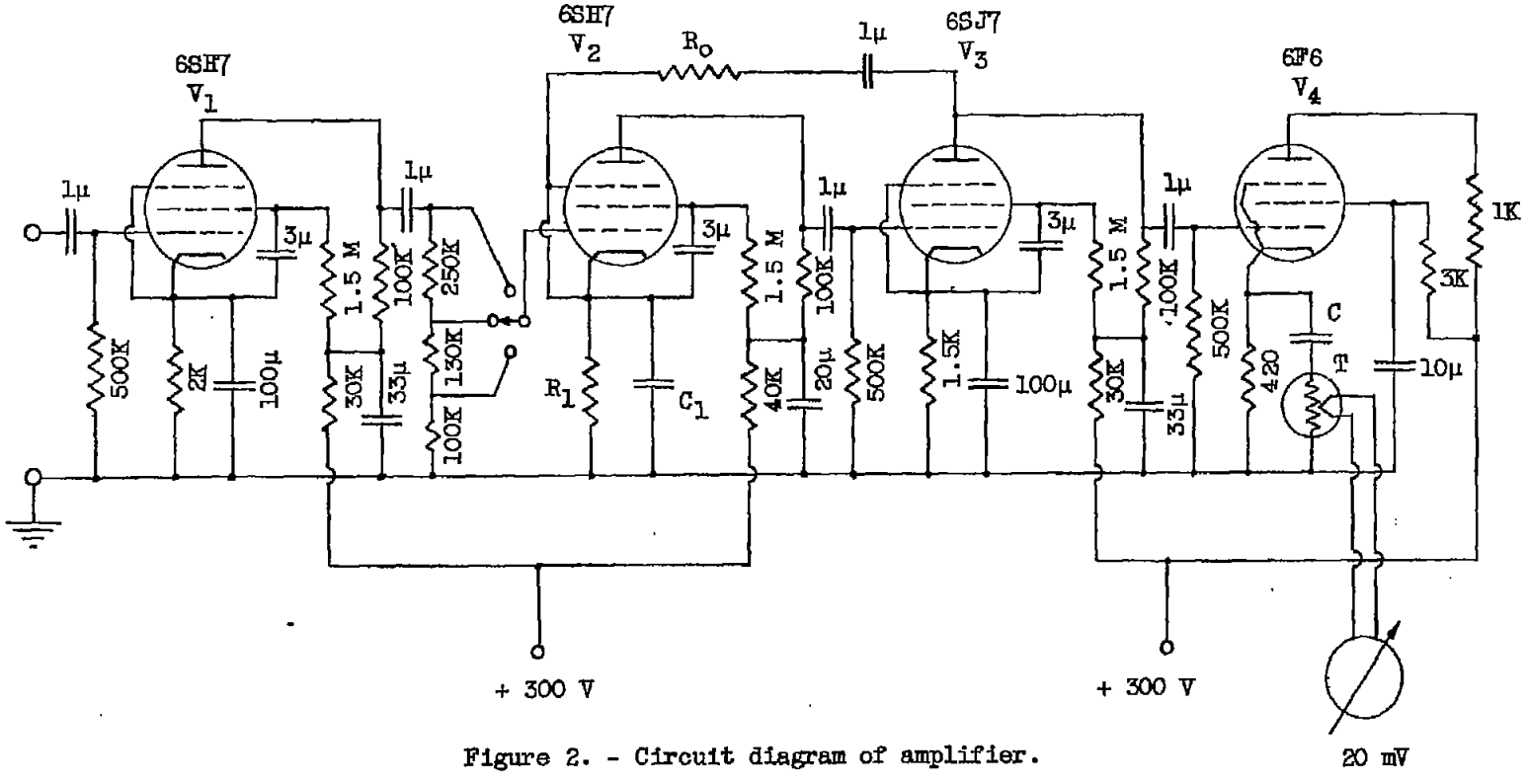


Figure 2. - Circuit diagram of amplifier.

C , 100μF; $R_o$ , 250 k Ω ;

$C_1$ , 10μF; $R_1$ , 2.3 k Ω .

4826

CD-2 back

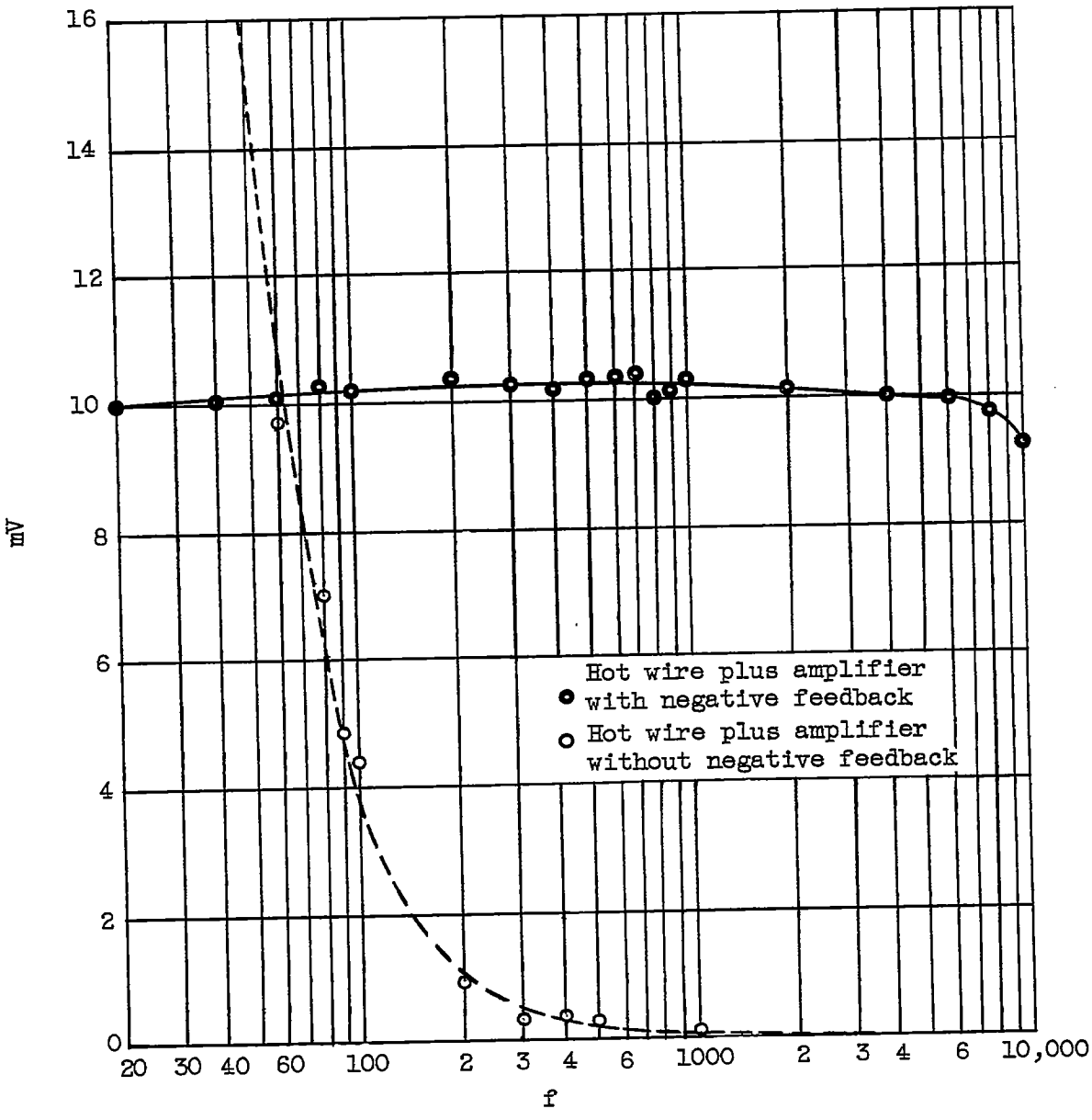


Figure 3. - Frequency characteristics.

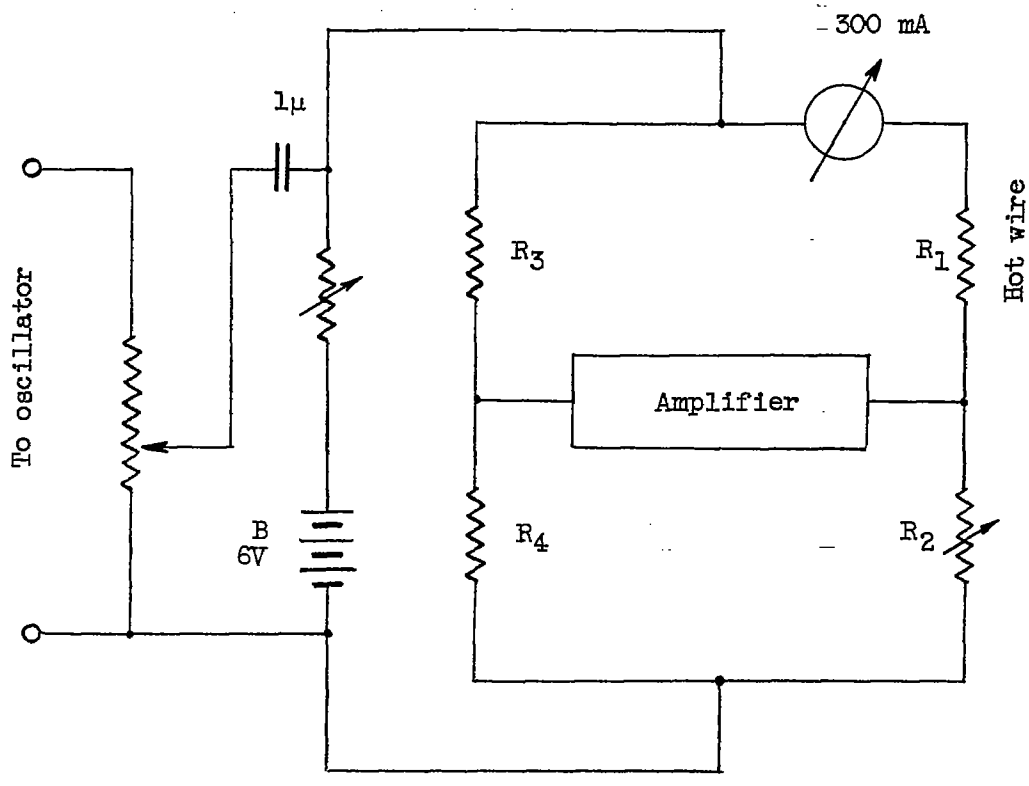


Figure 4. - Circuit diagram for determining frequency characteristics. A, low frequency signal generator; B, amplifier; C, hot wire.

4826

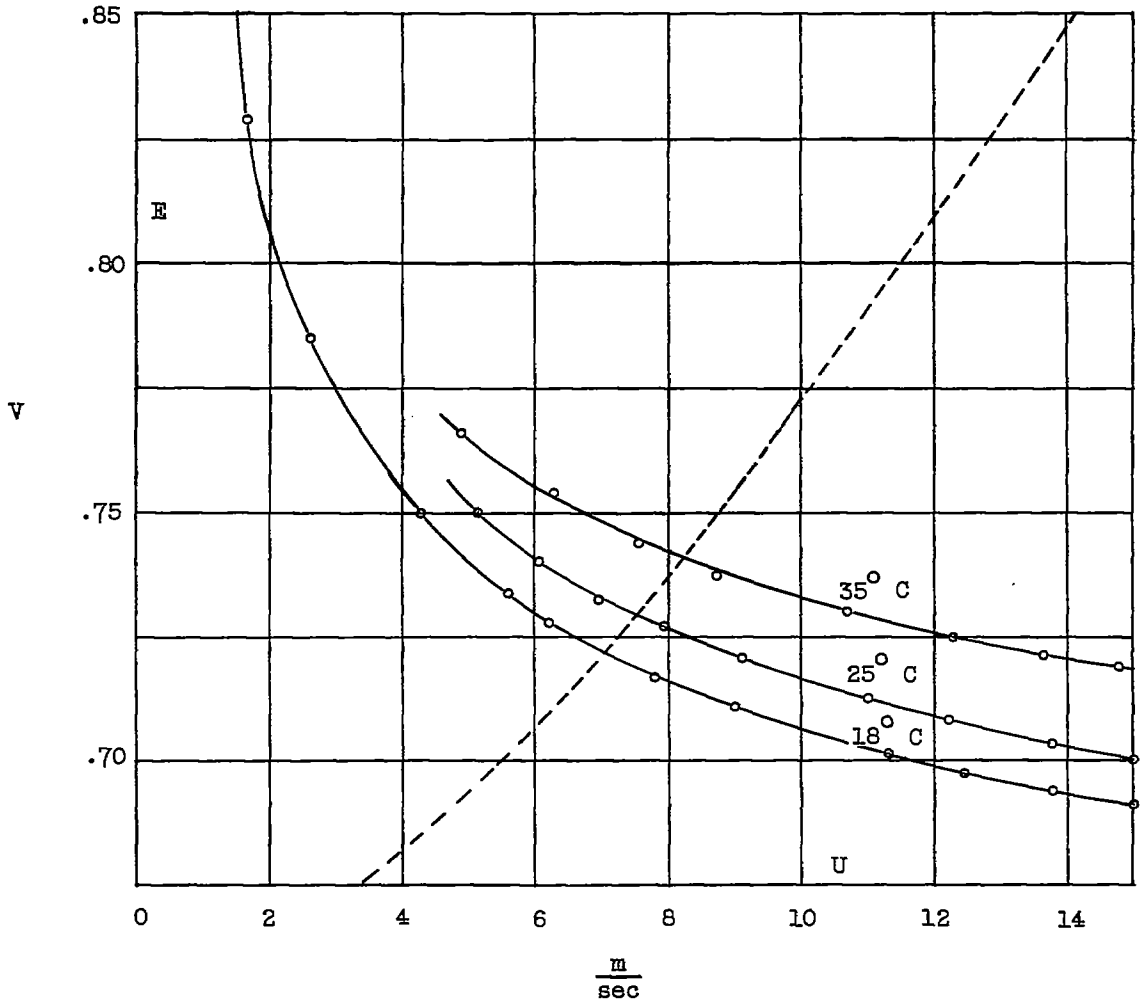


Figure 5. - Relation between mean velocity and voltage E.

4826

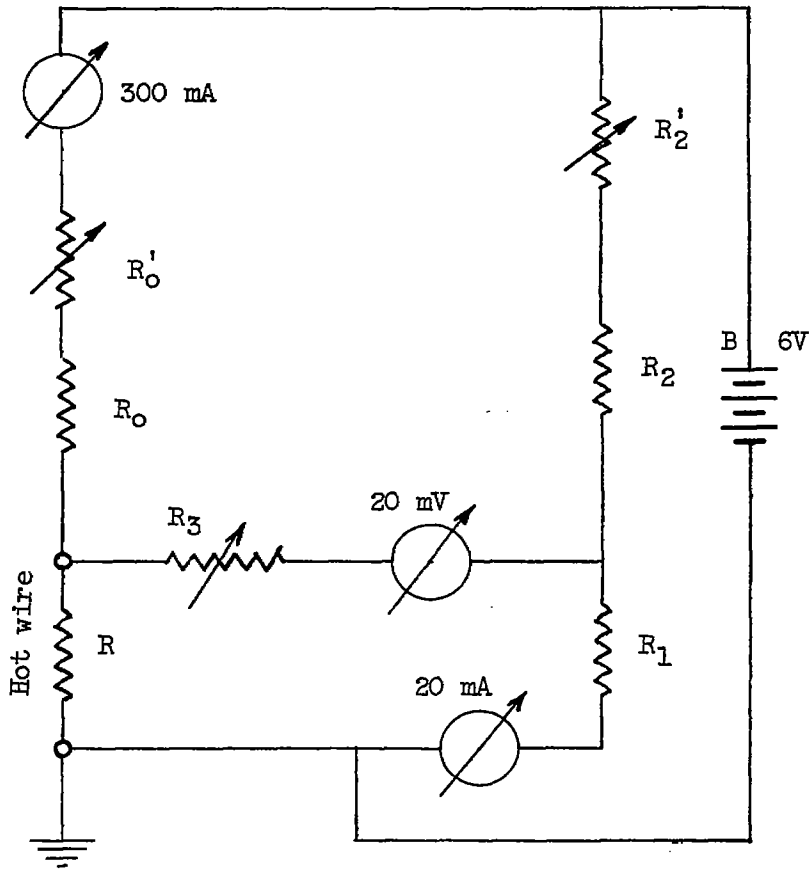


Figure 6. - Circuit diagram for measuring mean velocity.

4826

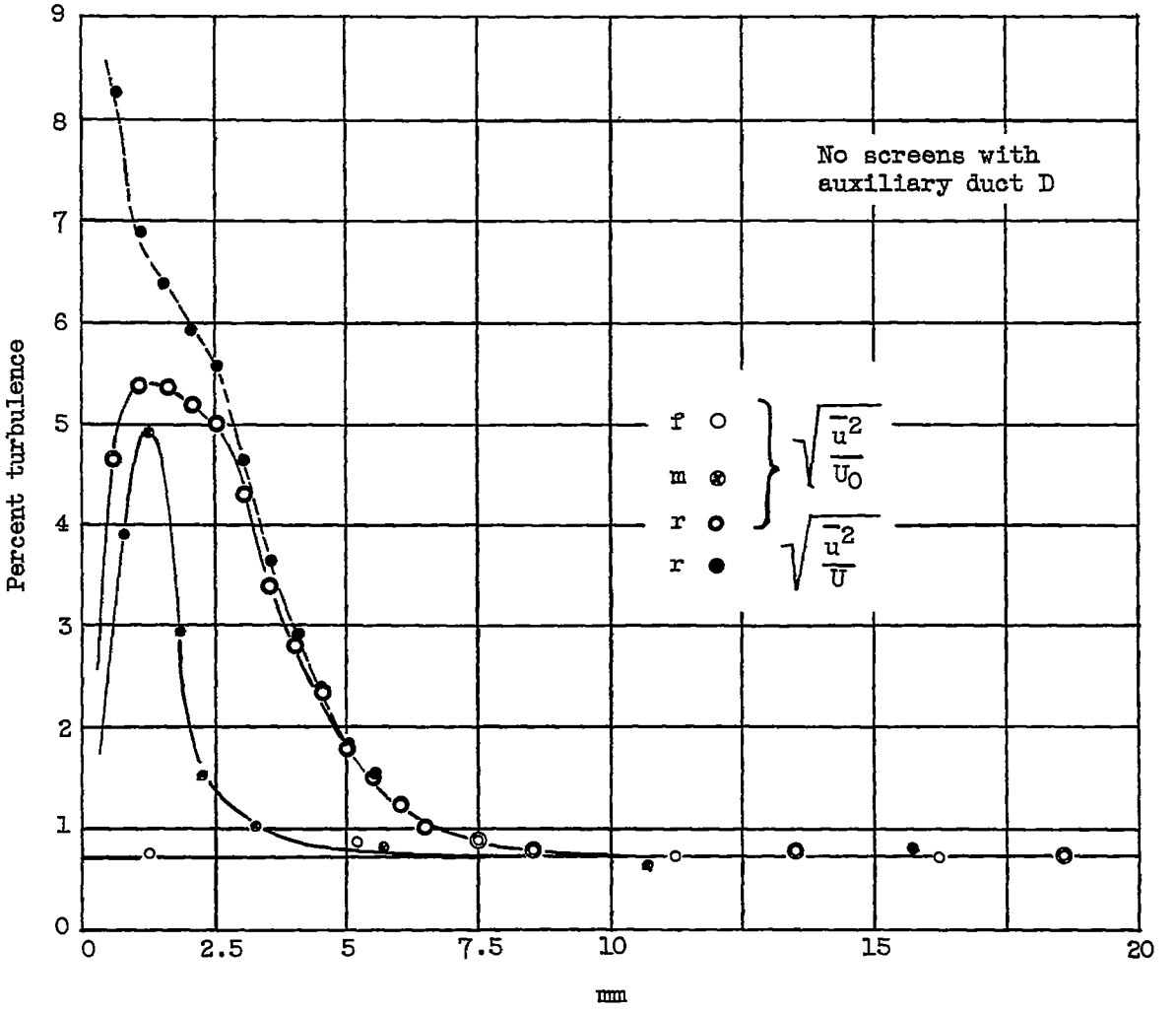


Figure 7. - Turbulence distribution in boundary layer. (No screen, no auxiliary duct.)

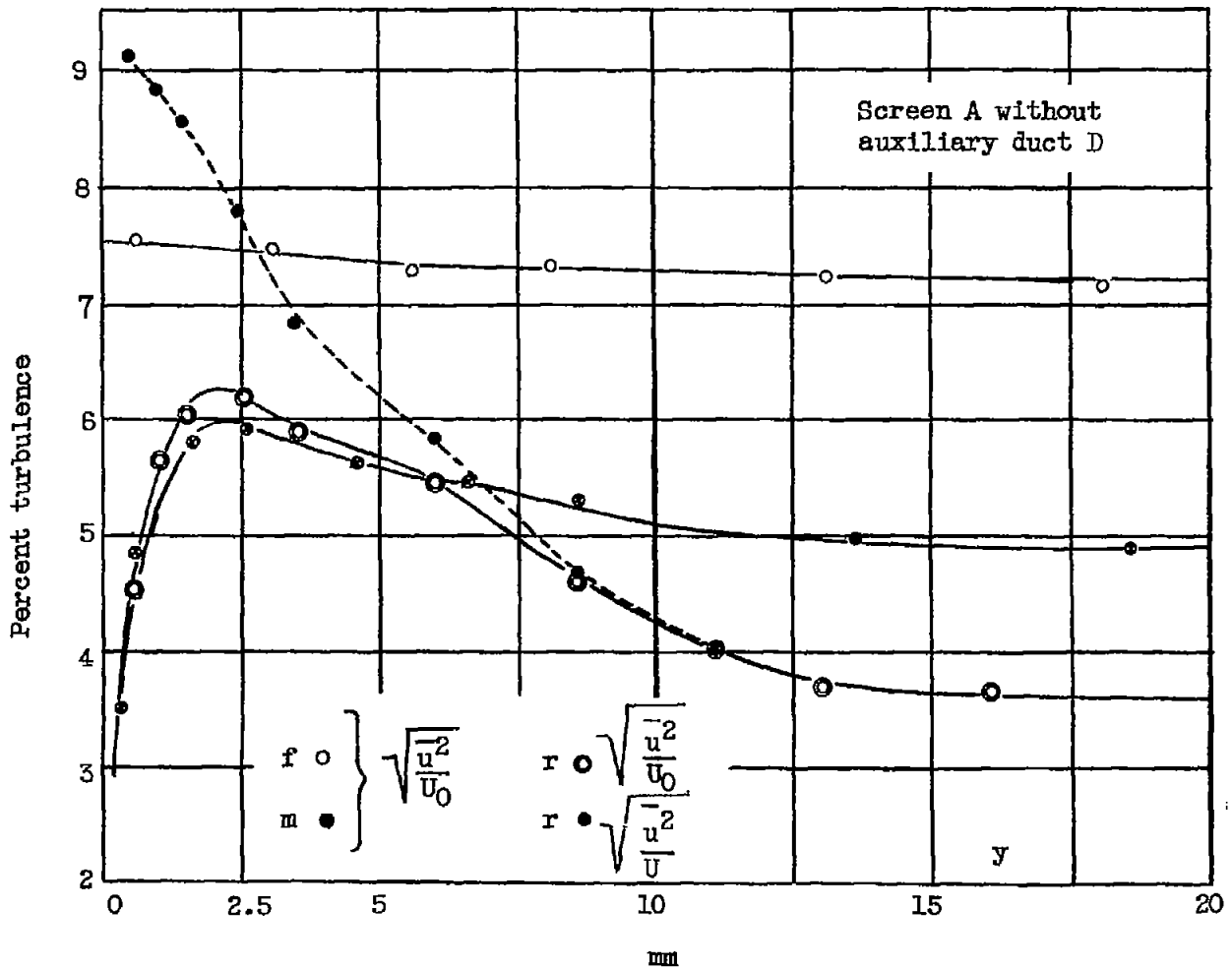


Figure 8. - Turbulence distribution in the boundary layer. (Screen A, no auxiliary duct.)

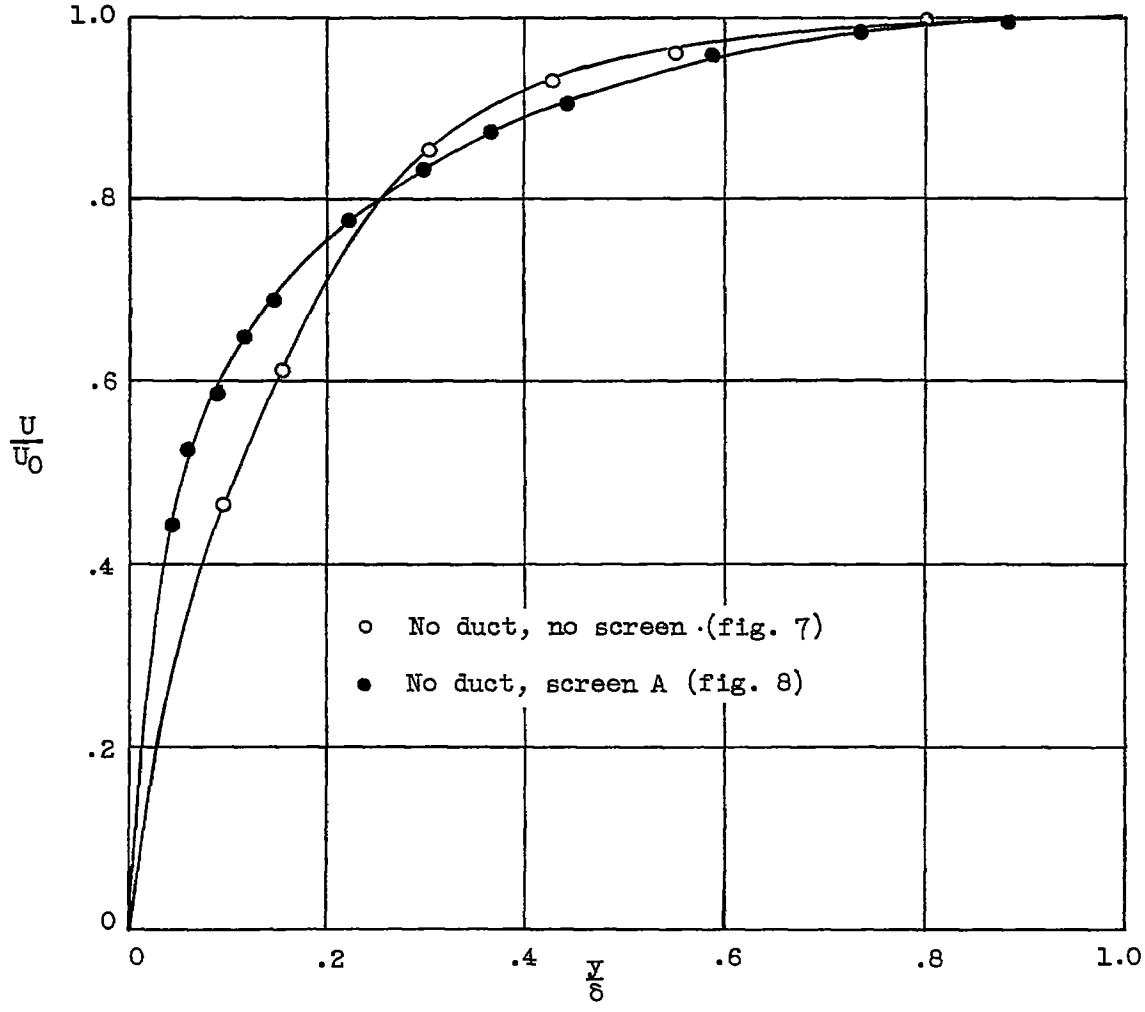


Figure 9. - Velocity profile in boundary layer at the middle of plate.

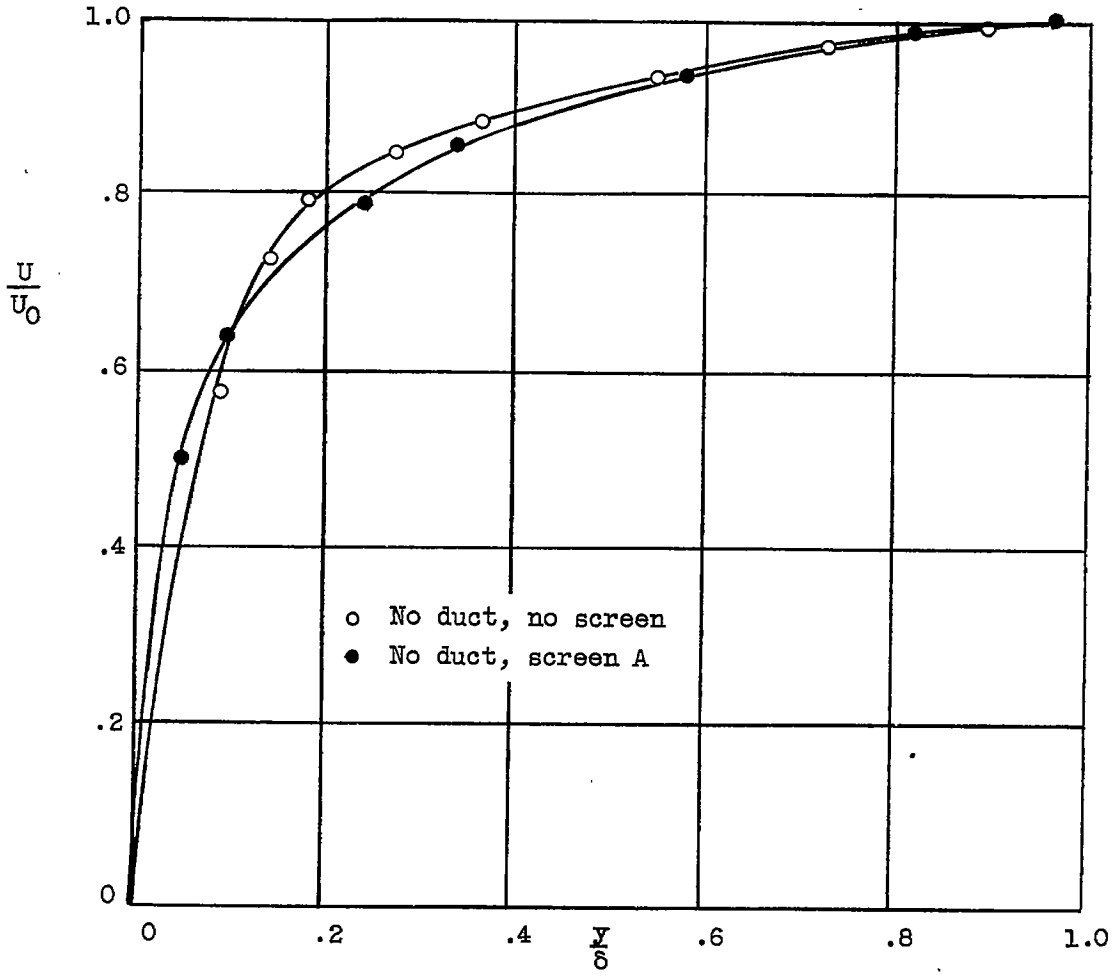


Figure 10. - Velocity profile in boundary layer near the rear end of plate.

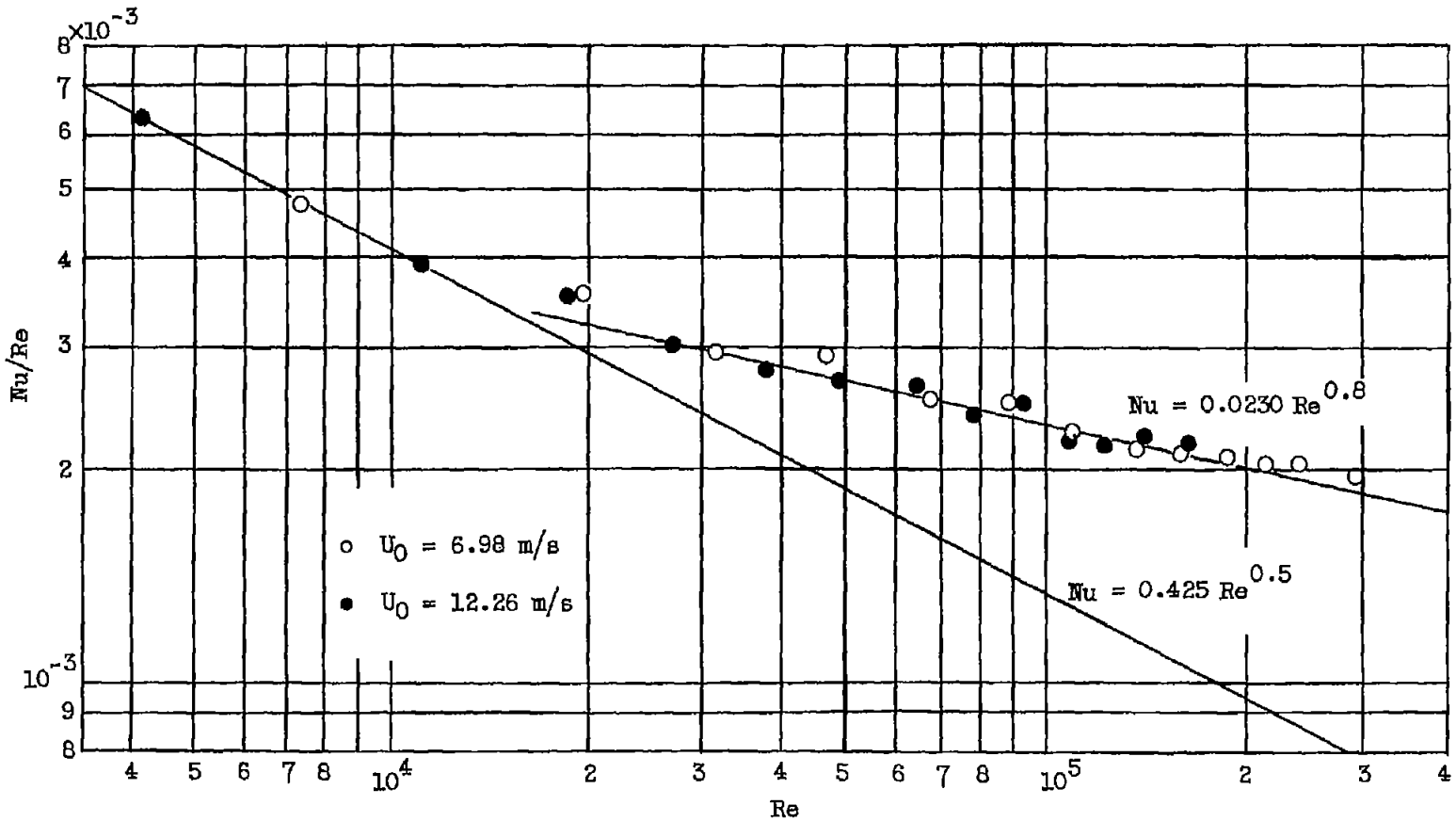


Figure 11. - Relation between Nu/Re and Re (screen A; duct, 50 cm.)

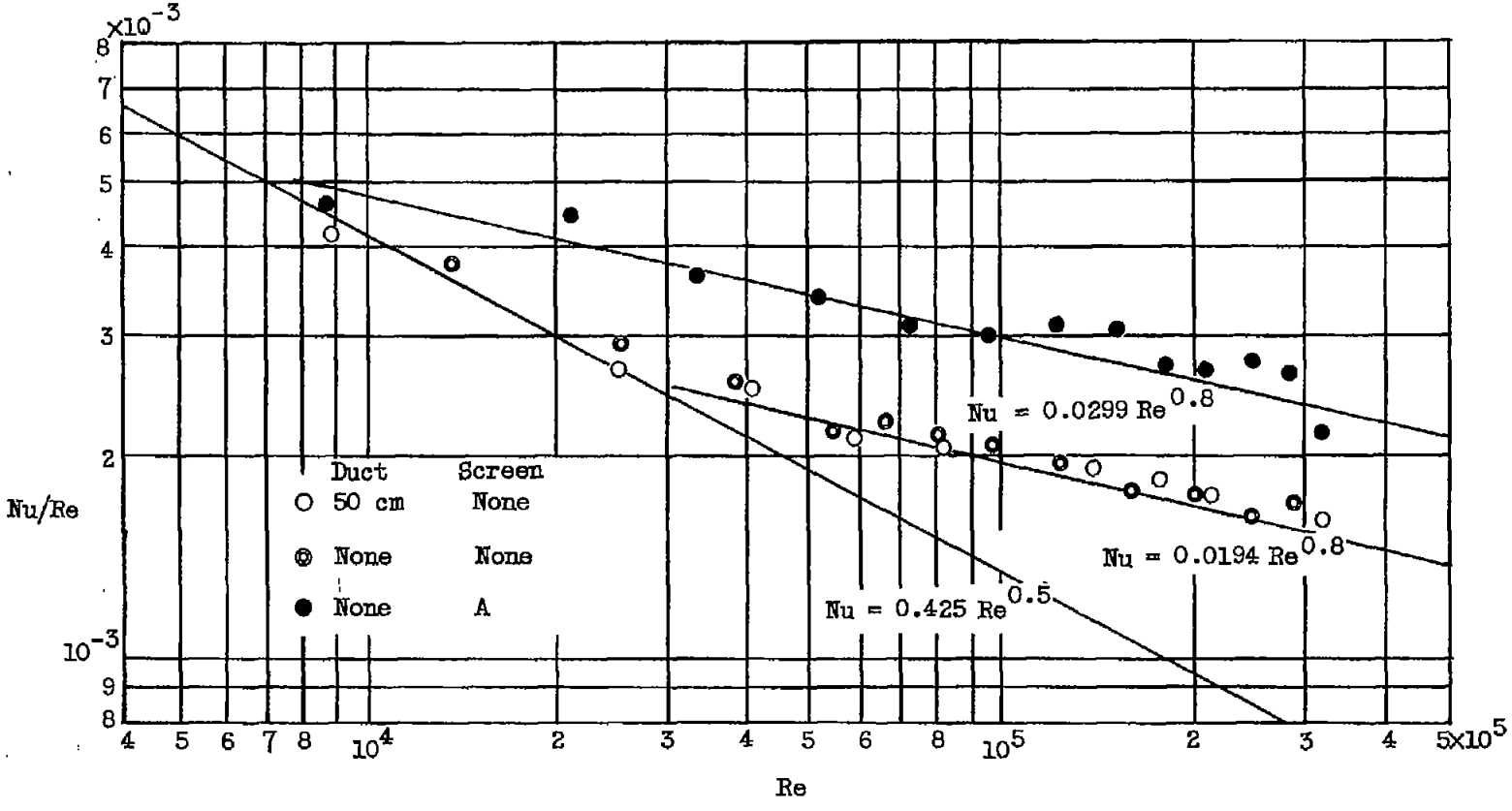


Figure 12. - Relation between Nu/Re and Re.

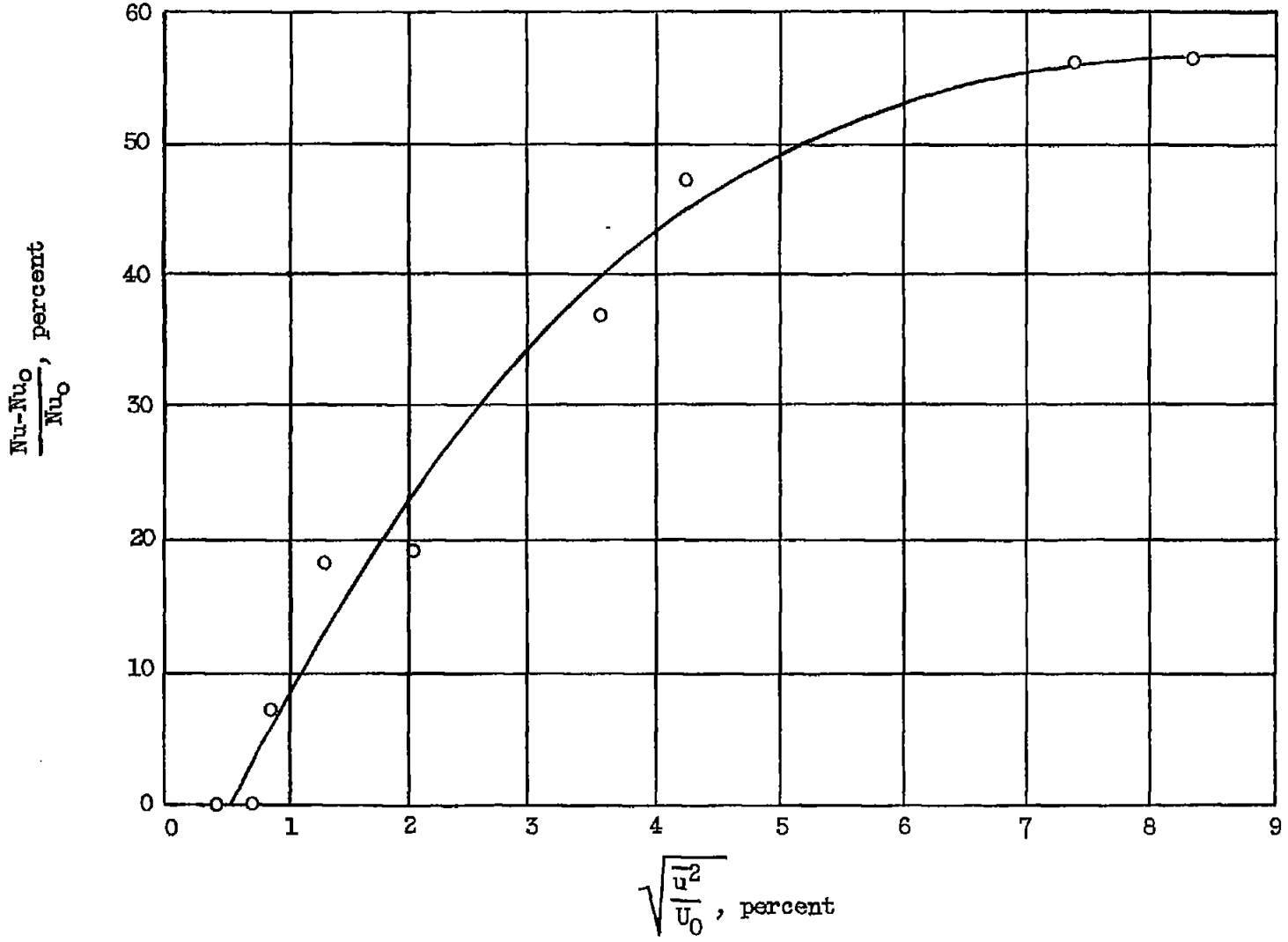


Figure 13. - Relation between increase of Nu and percentage of turbulence.



NACA - Langley Field, Va.